

See discussions, stats, and author profiles for this publication at: <https://www.researchgate.net/publication/50302970>

Interfacial Antiwear and Physicochemical Properties of Alkylborate–dithiophosphates

ARTICLE *in* ACS APPLIED MATERIALS & INTERFACES · MARCH 2011

Impact Factor: 6.72 · DOI: 10.1021/am101203t · Source: PubMed

CITATIONS

20

READS

59

5 AUTHORS, INCLUDING:



Faiz Ullah Shah

Luleå University of Technology

15 PUBLICATIONS 171 CITATIONS

SEE PROFILE



Sergei Glavatskih

KTH Royal Institute of Technology

64 PUBLICATIONS 659 CITATIONS

SEE PROFILE



Erik Höglund

Luleå University of Technology

36 PUBLICATIONS 390 CITATIONS

SEE PROFILE



Oleg N Antzutkin

The University of Warwick

144 PUBLICATIONS 4,651 CITATIONS

SEE PROFILE

Interfacial Antiwear and Physicochemical Properties of Alkylborate-dithiophosphates

Faiz Ullah Shah,[†] Sergei Glavatskih,^{*,‡} Erik Höglund,[‡] Mats Lindberg,[†] and Oleg N. Antzutkin^{*,†,§}

[†]Chemistry of Interfaces, Luleå University of Technology, S-97187 Luleå, Sweden

[‡]Division of Machine Elements, Luleå University of Technology, S-97187 Luleå, Sweden

[§]Department of Physics, University of Warwick, CV4 7AL Coventry, United Kingdom

 Supporting Information

ABSTRACT: Boron compounds have become of interest in tribology because of their unique tribochemical and tribological properties. At the same time, dialkyldithiophosphates (DTPs) of transition metals have been extensively used as multifunctional additives in lubricants to control friction and reduce wear in mechanical systems. Because of the environmental pollution and health hazards of these compounds, ashless compounds with reduced amounts of sulfur and phosphorus are desirable. This work reports on the synthesis, characterization, and tribological properties of a new class of compounds, alkylborate-dithiophosphates. This class combines two high-iron-affinity surface active groups, borate and dialkyldithiophosphate, into a single molecule. The final products, viscous liquids, were characterized by FT-IR, multinuclear ^1H , ^{13}C , ^{31}P , and ^{11}B NMR spectroscopy and thermal analyses. Residues of one representative compound from this class, DPB-EDTP, after thermal analyses were additionally characterized by multinuclear ^{13}C , ^{31}P and ^{11}B MAS and ^{31}P CP/MAS NMR spectroscopy. Solid-state NMR data suggest that a dominant part of the solid residue of DPB-EDTP consists of borophosphates. Antiwear and friction properties of a mineral oil with these novel additives were evaluated in a four-ball tribometer in comparison with *O,O'*-di-*n*-butyl-dithiophosphatozinc(II), Zn-BuDTP, as a reference lubricant additive. The surface morphology and the elemental composition of the tribofilms were characterized using scanning electron microscopy with energy-dispersive X-rays spectroscopy (SEM/EDS). The results show that alkylborate-dithiophosphates, with substantially reduced amounts of sulfur and phosphorus compared with Zn-BuDTP, have considerably better antiwear and friction performance.

KEYWORDS: dialkylborate-alkyl-dialkyldithiophosphates, lubricant additives, Zn-BuDTP, thermal analyses, borophosphates, solid-state MAS NMR, SEM/EDS

INTRODUCTION

Various compounds containing boron, phosphorus, sulfur, nitrogen, halogens, and metals have been used as additives in lubricants for several decades to minimize wear, control friction, improve efficiency and generally prolong machine service life. In boundary or mixed lubrication, under extreme conditions of high load and temperature, these additives undergo decomposition forming protective tribofilms through chemical reactions or adsorption processes. Thin tribofilms prevent direct metal-to-metal contact, welding of surface asperities, thus reducing wear.^{1–5} Wear is undesirable in practical applications, because it adversely affects functionality and limits the life-span of many mechanical devices with moving parts. The efficiency of additives depends on the ability to form a sufficiently hard and adhesive protective film on the sliding surfaces. This ability is related to their action mechanism, namely physical adsorption, chemisorption or chemical reactions with metals. The action mechanism of different additives changes for different metals and surface coatings. Additive performance depends on: (i) the polarity of its functional groups and its affinity to surface active sites, (ii) a composition of chemically

active elements, (iii) the reactivity of the decomposition products and (iv) the chemical activity of the metal surfaces.^{6–10}

Tribochemical reactions of additives with surfaces are generally catalyzed by the contact asperity temperature and the nascent metal surfaces. The contact temperature (also called “flash temperature”) can be very high (>400 °C) but it lasts for only a short time period (<millisecond). The nascent surfaces also possess a high surface energy and a large number of surface active sites. A rise in the contact temperature is caused by heat produced in the course of friction between the sliding asperities.¹¹ A variety of chemical reactions nearby the contacting surfaces may occur because of a combined effect of both heat and reactivity of the surface active sites and layers. These reactions are: (i) oxidation of the surfaces, (ii) oxidation and degradation of the lubricant, (iii) surface catalysis, (iv) polymerization and formation of layers of inorganic and organometallic products of decomposition of

Received: April 22, 2010

Accepted: March 7, 2011

Published: March 07, 2011

the additives.¹² The nature of inorganic and organometallic products formed on the surface depends on the reactivity, structure and composition of the additive. A high rate, at which tribofilms are formed (ca. 10–30 min), may also be explained by pressure-induced bulk effects. It has been shown with nanometer resolution that the tribofilms on top of surface asperities, which experience high contact pressure, are harder than those between the asperities.¹³

Zinc dialkyldithiophosphates (ZnDTPs) have been the additives of choice to provide protection against wear since the 1940s.^{14–17} Recently, environmental implications of using ZnDTPs have been addressed and the desire to use more environmentally friendly oil additives has become ever more apparent.¹⁸ It has been observed that ZnDTPs may cause eye irritation or, contact dermatitis and are mutagenic.^{19,20} These additives contain zinc, and large amounts of sulfur and phosphorus, which impair the environment indirectly by poisoning emission-control catalysts and by blocking filters in car exhaust systems.²¹ Because of significant health, economic, and environmental issues, significant efforts are being made to develop and implement lubricants that contain smaller amounts of S and P without metals. Finding an efficient and environmentally friendly replacement of ZnDTP by zinc-free, low-sulfur, and low-phosphorus additives is of great interest in tribochemical research.

Interest in boron compounds for various applications is increasing because of the unique combination of chemical and tribological properties of these compounds. Specifically, boron compounds have been extensively studied as soluble additives in lubricating oils, as solid lubricants and as surface coatings. Oil soluble organoboron compounds are promising friction modifiers, corrosion inhibitors, antioxidants and effective antiwear additives.^{22,23} To reduce the amounts of sulfur and phosphorus in lubricants and to enhance their tribological performance, ZnDTPs in combination with different borate additives have been widely studied. Combinations of ZnDTP with potassium triborate,²⁴ calcium borate,²⁵ or boric additive²⁶ have exhibited improved antiwear properties. Combinations of boron and sulfur in a single molecule such as borate with mercaptobenzothiozole²⁷ or dithiocarbamates²⁸ have also shown improved antiwear performance. Previous reports suggest that a combination of thiophosphate with borate compounds as additives does improve antiwear performance of lubricants in the boundary lubrication regime. Therefore, it is anticipated that designing novel compounds, in which elements B, P, and S in different triboactive groups are combined “intra-molecularly” in one molecule, may lead to lower optimum concentrations of these novel additives in base oils compared to the oil formulations with “inter-molecular” mixtures of additives.

Boron containing compounds are believed to be an attractive alternative for commercially available lubricant additives.²⁹ It is known that boron, boron nitride, and metal boride are very hard materials.^{30,31} Rhodium and iridium boride films are known to be superhard with intrinsic hardness of 44 and 43 GPa, respectively.³² Recently, it was found that rhenium boride (ReB₂) synthesized in mild chemical conditions has an average hardness of 48 GPa, which is even larger than this for boron nitride materials.³³ Therefore, hard iron boride phases (Fe₂B) can also be formed on steel surface nanosize asperities under mildly elevated local temperature (300–400 °C) and pressure in boundary lubrication.³⁴ A hard metal boride layer on a steel surface is, probably, additionally supported by a glassy boron-phosphate layer, which can also be formed in the tribofilm. Both layers provide an additional antiwear benefit by protecting metal surfaces from damage during sliding motion in tribological applications.

In this work we report on the synthesis, characterization and tribological study of a new class of lubricant additives, alkylborate-dithiophosphates. The main goal of this study is to combine B, S and P atoms in one organic molecule aiming at improving tribological and environmental performance of both dialkyldithiophosphates and borate esters. In comparison to *S*-di-*n*-octoxyboron-*O,O'*-di-*n*-octyldithiophosphate with a direct S–B chemical bond,³⁵ in these novel compounds, boron was covalently bonded to the dialkyldithiophosphate group through the ethyl linker in order to avoid hydrolysis of the direct boron–sulfur bond by traces of moisture usually present in lubricating oils. Performance of alkylborate-dithiophosphates was evaluated in comparison with *O,O'*-di-*n*-butyl-dithiophosphato-zinc(II) (Zn-BuDTP), at concentrations 0.1–1.0 wt % in a mineral oil. In addition, solid-state multinuclear ¹³C, ³¹P, and ¹¹B MAS NMR was performed on residues of *S*-(di-*n*-pentylborate)-ethyl-*O,O'*-di-*n*-pentyldithiophosphate (DPB-EDTP) after thermal analyses in order to get deeper insights into the chemical nature of these residues and a sequence of cleavage of chemical bonds in DPB-EDTP upon heating. These measurements reveal physicochemical changes that occur during the thermal decomposition of DPB-EDTP and on how the decomposition products may influence the tribological performance of this novel additive, when a tribofilm is formed on steel surfaces.

EXPERIMENTAL SECTION

Chemicals. Phosphorus pentasulfide, P₂S₅ (Aldrich, 99% purity), pentanol (Prolabo, 98% purity), 2-chloroethanol (Fluka, >99% purity), boric acid (Merck, analytical grade), sodium sulfate (Merck, analytical grade), potassium hydroxide pellets (Merck, analytical grade) and toluene (Fluka, > 99.7% purity) were used as received. *O,O'*-Di-*n*-butyl-dithiophosphato-zinc(II) (Zn-BuDTP, MW. 548.04) was synthesized as previously reported.³⁶ This compound is a viscous liquid at room temperature and it is easily miscible with the base oil used in this study. The purity of Zn-BuDTP complex and its corresponding potassium salt was checked by ³¹P NMR. (145.70 MHz, δ): 100.29 ppm³⁷ and ³¹P NMR for potassium salt (145.70 MHz, ethanol, δ) 112.72 ppm.

Synthesis of Alkylborate-dithiophosphates. Three dialkylborate-dithiophosphates with different lengths of the alkyl chain were synthesized.

***S*-(di-*n*-pentylborate)-ethyl-*O,O'*-di-*n*-pentyldithiophosphate (DPB-EDTP).** Step 1: Phosphorus pentasulfide (4.44 g, 20 mmol) was suspended in toluene (100 mL) and pentanol (80 mmol) was added gradually. The reaction mixture was stirred at 80–100 °C for 3 h. The suspension was filtered to remove unreacted phosphorus pentasulfide (P₂S₅). 40 mmol of potassium hydroxide was added in the form of 50% aqueous solution with continuous stirring at room temperature. Toluene and water were removed and the crude product was dried. The crude potassium *O,O'*-di-*n*-pentyldithiophosphate was washed with hexane (yield 75%).

FT-IR (KBr, cm^{−1}, powder): 2957, 2873 ν (C–H, stretching); 983 ν (P–OC, medium); 708 ν (P=S, medium); 548 ν (P–S, medium).

³¹P NMR (145.70 MHz, ethanol, δ): 112.79 ppm.

Step 2: 20 mmol (1.61 g) of chloroethanol was added to an aqueous suspension of potassium salt of *O,O'*-di-*n*-pentyldithiophosphate (20 mmol, 6.16 g) with constant stirring. The resulting reaction mixture was refluxed for 3 h. A new formed organic layer was extracted with toluene from the aqueous phase, washed with water several times, dried over anhydrous sodium sulfate and filtered. Traces of solvent and water were removed in a rotary evaporator to give *S*-hydroxyethyl-*O,O'*-di-*n*-pentyldithiophosphate, (4.64 g, 74% yield).

FT-IR (KBr, cm^{-1}): 3427 $\nu(\text{O}-\text{H}$, broad); 2927, 2858 $\nu(\text{C}-\text{H}$, stretching); 980 $\nu(\text{P}-\text{OC}$, medium); 729 $\nu(\text{P}=\text{S}$, medium); 662 $\nu(\text{P}-\text{S}$, medium).

^1H NMR (359.93 MHz, CDCl_3 , δ): 0.91 (6H, t, $^3J_{\text{HH}} = 6.54$ Hz, CH_3); 1.32–1.40 (8H, m, $-\text{CH}_2-$); 1.68–1.76 (4H, m, $\text{CH}_2\text{CH}_2\text{OP}$); 2.21 (1H, s, OH); 3.09 (2H, dt, $^3J_{\text{HP}} = 18.65$, $^3J_{\text{HH}} = 5.76$, CH_2S); 3.85 (2H, t, $^3J_{\text{HH}} = 6.04$ Hz, CH_2OH); 4.04–4.18 (4H, m, CH_2OP).

^{13}C NMR (90.57 MHz, CDCl_3 , δ): 14.05 ($2 \times \text{CH}_3$); 22.30 ($2 \times \text{CH}_2-\text{CH}_3$); 27.82, 29.80, ($4 \times -\text{CH}_2-$); 36.46 ($1 \times \text{CH}_2-\text{S}$); 62.04 ($1 \times \text{CH}_2-\text{O}-\text{B}$); 68.37 ($2 \times \text{CH}_2-\text{O}-\text{P}$) ppm.

^{31}P NMR (145.70 MHz, CDCl_3 , δ): 96.25 ppm.

Step 3: A solution of 10 mmol (3.14 g) of *S*-hydroxyethyl-*O*,*O'*-di-*n*-pentylthiophosphate in 80 mL of toluene was placed together with 10 mmol (0.618 g) of boric acid and 20 mmol of primary pentanol in a 250 mL round-bottom flask equipped with a magnetic stirrer, a condenser, and a water separator (prebaked on vacuum to exclude any moisture). The reaction mixture was refluxed for 6 h under nitrogen atmosphere; water was continuously removed from the reaction mixture. The reaction mixture was rotary evaporated to remove the solvent. Residual amounts of solvent and pentanol were removed by heating the crude product at 0.2 mmHg, 120 °C for 30 min. A transparent viscous liquid product, *S*-(di-*n*-pentylborate)-ethyl-*O*,*O'*-di-*n*-pentylthiophosphate was obtained in 89% yield (4.42 g).

Anal. Calcd for $\text{C}_{22}\text{H}_{48}\text{O}_5\text{PS}_2\text{B}$ (MW, 498.46): C, 53.0; H, 9.7; B, 2.2. Found: C, 52.3; H, 9.7; B, 2.6.

FT-IR (KBr, cm^{-1}): 2957, 2932, 2873 $\nu(\text{C}-\text{H}$, CH_3 stretching); 984 $\nu(\text{P}-\text{OC}$, medium); 730 $\nu(\text{P}=\text{S}$, medium); 666 $\nu(\text{P}-\text{S}$, medium).

^1H NMR (359.93 MHz, CDCl_3 , δ): 0.91 (6H, t, $^3J_{\text{HH}} = 7.0$ Hz, CH_3); 0.90 (6H, t, $^3J_{\text{HH}} = 6.94$ Hz, CH_3); 1.30–1.40 (16H, m, $-\text{CH}_2-$); 1.49–1.57 (4H, m, $\text{CH}_2\text{CH}_2\text{OB}$); 1.68–1.75 (4H, m, $\text{CH}_2\text{CH}_2\text{OP}$); 3.01 (2H, dt, $^3J_{\text{HP}} = 16.37$, $^3J_{\text{HH}} = 6.56$, CH_2S); 3.76 (4H, t, $^3J_{\text{HH}} = 6.64$ Hz, CH_2OB , pentyl chain); 3.96 (2H, t, $^3J_{\text{HH}} = 6.49$ Hz, CH_2OB , ethyl); 4.02–4.18 (4H, m, CH_2OP).

^{13}C NMR (90.57 MHz, CDCl_3 , δ): 14.20 ($2 \times \text{CH}_3$); 14.06 ($2 \times \text{CH}_3$); 22.57 ($2 \times \text{CH}_2-\text{CH}_3$); 22.36 ($2 \times \text{CH}_2-\text{CH}_3$); 27.86, 28.15, 29.84, 31.37 ($8 \times \text{CH}_2$, pentyl chains); 34.79 ($1 \times \text{CH}_2-\text{S}$); 63.34 ($3 \times \text{CH}_2-\text{O}-\text{B}$); 68.03 ($2 \times \text{CH}_2-\text{O}-\text{P}$) ppm.

^{31}P NMR (145.70 MHz, CDCl_3 , δ): 95.91 ppm.

^{11}B NMR (115.48 MHz, CDCl_3 , δ): 17.59 ppm.

***S*-(Di-*n*-octylborate)-ethyl-*O*,*O'*-di-*n*-octylthiophosphate (DOB-EDTP).** The procedure is similar to that used in the synthesis of DPB-EDTP. The final product, a transparent viscous liquid of DOB-EDTP was obtained in yield 90%. Anal. Calcd for $\text{C}_{34}\text{H}_{72}\text{O}_5\text{PS}_2\text{B}$ (MW, 666.75): C, 61.3; H, 10.9; B, 1.62; P, 4.64; S, 9.62. Found: C, 63.5; H, 11.3; B, 1.58; P, 3.79; S, 8.57.

FT-IR (KBr, cm^{-1}): 2956, 2927, 2856 $\nu(\text{C}-\text{H}$, stretching); 1337 $\nu(\text{B}-\text{O}$, stretching); 987 $\nu(\text{P}-\text{OC}$, stretching); 729 $\nu(\text{P}=\text{S}$, stretching); 666 $\nu(\text{P}-\text{S}$, stretching).

^1H NMR (359.929 MHz, CDCl_3 , δ): 0.88 (12H, t, $^3J_{\text{HH}} = 6.37$ Hz, CH_3); 1.26–1.40 (40H, m, $-\text{CH}_2-$); 1.48–1.56 (4H, m, $\text{CH}_2\text{CH}_2\text{OB}$); 1.67–1.75 (4H, m, $\text{CH}_2\text{CH}_2\text{OP}$); 3.01 (2H, dt, $^3J_{\text{HP}} = 16.65$, $^3J_{\text{HH}} = 6.37$, CH_2S); 3.76 (4H, t, $^3J_{\text{HH}} = 6.50$ Hz, CH_2OB , octyl chains); 3.96 (2H, t, $^3J_{\text{HH}} = 6.42$ Hz, CH_2OB , ethyl); 4.01–4.18 (4H, m, CH_2OP).

^{13}C NMR (90.567 MHz, CDCl_3 , δ): 14.26 (q, $4 \times \text{CH}_3$); 22.84 (t, $4 \times \text{CH}_2-\text{CH}_3$); 26.01, 28.15, 29.52, 30.70, 32.01 (t, $20 \times \text{CH}_2$, octyl chains); 34.85 (t, $1 \times \text{CH}_2-\text{S}$); 63.41 (t, $3 \times \text{CH}_2-\text{O}-\text{B}$); 68.09 (t, $2 \times \text{CH}_2-\text{O}-\text{P}$) ppm.

^{31}P NMR (145.70 MHz, CDCl_3 , δ): 95.88 ppm.

^{11}B NMR (115.48 MHz, CDCl_3 , δ): 17.52 ppm.

***S*-(Di-*n*-decylborate)-ethyl-*O*,*O'*-di-*n*-decylthiophosphate (DDB-EDTP).** The procedure is similar to that used in the synthesis of DPB-EDTP. DDB-EDTP is a transparent viscous liquid at room temperature (yield 92%). Anal. Calcd for $\text{C}_{42}\text{H}_{88}\text{O}_5\text{PS}_2\text{B}$ (MW, 779.02): C, 64.6; H, 11.4; B, 1.40; P, 3.97; S, 8.23. Found: C, 67.6; H, 11.8; B, 1.64; P, 2.83; S, 7.82.

FT-IR (KBr, cm^{-1}): 2955, 2926, 2855 $\nu(\text{C}-\text{H}$, stretching); 1337 $\nu(\text{B}-\text{O}$, stretching); 989 $\nu(\text{P}-\text{OC}$, stretching); 729 $\nu(\text{P}=\text{S}$, stretching); 666 $\nu(\text{P}-\text{S}$, stretching).

^1H NMR (359.929 MHz, CDCl_3 , δ): 0.88 (12H, t, $^3J_{\text{HH}} = 6.51$ Hz, CH_3); 1.25–1.32 (56H, m, $-\text{CH}_2-$); 1.48–1.55 (4H, m, $\text{CH}_2\text{CH}_2\text{OB}$); 1.66–1.74 (4H, m, $\text{CH}_2\text{CH}_2\text{OP}$); 3.01 (2H, dt, $^3J_{\text{HP}} = 16.31$ Hz, $^3J_{\text{HH}} = 6.28$ Hz, CH_2S); 3.76 (4H, t, $^3J_{\text{HH}} = 6.45$ Hz, CH_2OB , decyl chains); 3.96 (2H, t, $^3J_{\text{HH}} = 6.42$ Hz, CH_2OB , ethyl); 4.02–4.18 (4H, m, CH_2OP).

^{13}C NMR (90.567 MHz, CDCl_3 , δ): 14.26 (q, $4 \times \text{CH}_3$); 22.88 (t, $4 \times \text{CH}_2-\text{CH}_3$); 24.26, 26.01, 28.38, 29.83, 30.96, 31.19, 32.10 (t, $28 \times \text{CH}_2$, decyl chains); 33.54 ($1 \times \text{CH}_2-\text{S}$); 63.38 (t, $3 \times \text{CH}_2-\text{O}-\text{B}$); 68.01 (t, $2 \times \text{CH}_2-\text{O}-\text{P}$) ppm.

^{31}P NMR (145.70 MHz, CDCl_3 , δ): 95.90 ppm.

^{11}B NMR (115.48 MHz, CDCl_3 , δ): 17.50 ppm.

Liquid- and Solid-State NMR. Liquid-state one-pulse NMR spectra of Zn-BuDTP, DPB-EDTP, DOB-EDTP, DDB-EDTP, and intermediates of syntheses were recorded in CDCl_3 (at 5–10 wt % of solutes) on a Varian/Chemagnetics InfinityPlus CMX-360 ($B = 8.46$ T) spectrometer using a 10 mm double-resonance probe for liquids tuned to resonance frequencies of ^1H (359.93 MHz), ^{13}C (90.57 MHz), ^{31}P (145.70 MHz) or ^{11}B (115.48 MHz). The following references were used: TMS for ^1H (internal reference), 77.2 ppm resonance peak of CDCl_3 for ^{13}C , H_3PO_4 (85%) as an external reference (0 ppm)³⁸ for ^{31}P , and $\text{Et}_2\text{O} \cdot \text{BF}_3$ as an external reference (0 ppm) for ^{11}B .³⁹

Solid-state multinuclear ^{13}C , ^{31}P and ^{11}B magic-angle-spinning (MAS) NMR spectra of residues of DPB-EDTP after TGA were recorded on the same spectrometer either in the one-pulse direct-excitation experiments (for ^{13}C , ^{31}P , and ^{11}B) or with cross-polarization (CP) from the protons and with a weak CW proton decoupling corresponding to the nutation frequency of protons 28 kHz (for ^{13}C and ^{31}P). For consistency, single-pulse ^{13}C NMR spectra of liquid DPB-EDTP (filled in a 4 mm glass vial) with a CW decoupling of 40 kHz were also obtained in the same 4 mm MAS probe. All spectra were externally referenced using either polycrystalline adamantane (38.48 ppm⁴⁰ relative to TMS (0 ppm)) or liquid samples of H_3PO_4 (85%) (0 ppm) for ^{31}P and $\text{Et}_2\text{O} \cdot \text{BF}_3$ (0 ppm) for ^{11}B , filled in small capillaries (1 mm in diameter) and inserted in empty rotors. A black solid (ca. 6 mg) or a white jelly-like (ca. 30 mg) sample of DPB-EDTP residues after TGA were packed in 4 mm standard ZrO_2 rotors and spun at 4–10 kHz.

For ^{11}B , the 90° pulse was 4.8 μs as calibrated using a liquid reference sample of $\text{Et}_2\text{O} \cdot \text{BF}_3$. Then, on solid samples, a “quadrupolar” (^{11}B , $I = 3/2$) excitation 45° pulse of 2.4 μs was used in the one-pulse experiments with a recycling delay of 10 s. Further experimental details are given in the figure legends.

^{31}P MAS NMR spectra were deconvoluted using in-built spectrometer software routines (“Spinsight”). A combination of 50% Gaussian and 50% Lorentzian broadening of the deconvoluted resonance lines gave the best fit to the experimental NMR spectra.

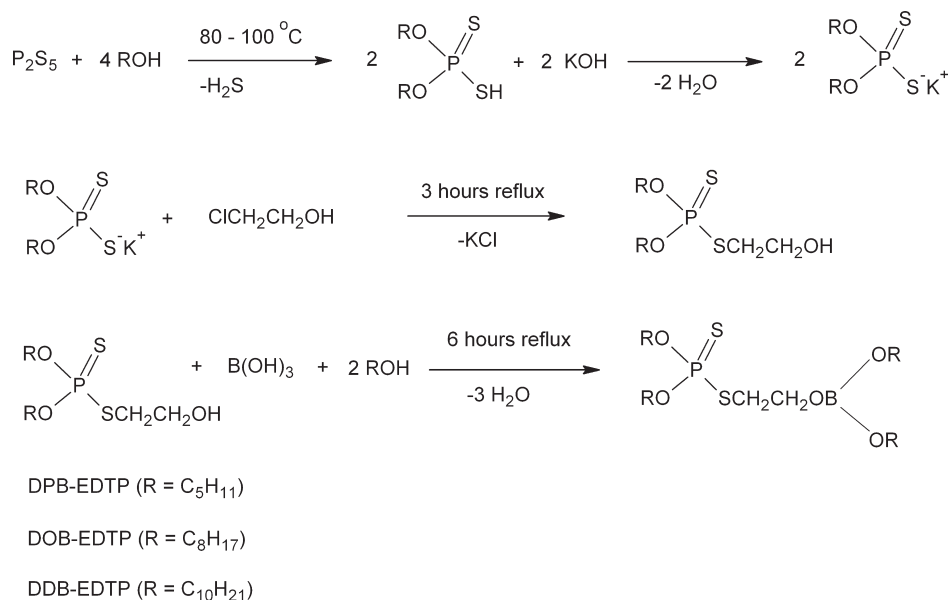
Physical, Thermal, and Surface Characterization. Elemental analysis for C and H was performed according to the Dumas method⁴¹ and elemental analysis of B was carried out using ICP-SFMS.⁴²

FT-IR spectra were recorded on a Perkin-Elmer 2000 spectrometer in the range 4000–370 cm^{-1} . Sampling was performed by placing a droplet of compound onto a KBr pellet.

Thermal analyses were performed by Netzsch STA 409 instrument equipped with simultaneous thermogravimetric (TG) and differential thermal analysis (DTA) at a rate of 20 °C/min and argon flow rate of 100 mL/min. The sensitivity of this STA Instruments is $\pm 1 \mu\text{g}$.

Scanning electron microscopy (SEM) studies were carried out using a Philips XL 30 scanning electron microscope (SEM) equipped with LaB6 emission source. A link ISIS Ge energy dispersive X-ray detector (EDS) attached to the SEM was used to additionally probe the composition of the entire tribofilm on the ball surfaces. Some SEM/EDS measurements

Scheme 1. Synthesis of Alkylborate-dithiophosphates



(for DOB-EDTP and DDB-EDTP) were performed using JEOL JSM-6460 (software INCA). Prior to the analysis, the balls were cleaned ultrasonically for 5 min with petroleum ether, in order to eliminate residual lubricant.

Tribological Performance. Additives were mixed with the base oil at fixed weight (%) concentrations of 0.1, 0.2, 0.4, 0.6, 0.8, and 1.0% using an analytical balance. The density and viscosity of the base oil are 0.8135 g·mL⁻¹ and 17.5 mPa s (at 40 °C) and 4.9 mPa s (at 100 °C), respectively. The elemental composition of the mineral oil used in this study is: carbon, 86.0 ± 0.7% and hydrogen, 14.5 ± 0.5%. The steel balls used in the tests were 12.7 mm in diameter with a surface hardness HRC 60–67. AISI 52100 steel composition: C, 0.95–1.10%; Si, 0.15–0.30%; Mn, <0.25%; P, <0.03%; S, <0.025%; Cr, 1.30–1.60%.

Friction and antiwear properties of these compounds as additives in the base oil were evaluated with a four-ball tribometer. Test conditions were as follows: rotational speed 1450 rpm, test duration time 30 min, load 392 N and temperature 294 K. The wear scar diameter (WSD) and the friction coefficient were studied as a function of the additive concentration (wt %). WSDs for the three lower stationary balls were measured using an optical profiler (WYKO NT 1100). The mean of these three WSDs and a mean of the statistical deviation (SD) were calculated and tabulated (see Table SI-27 in the Supporting Information). Before each test, the ball holder was washed with petroleum ether while the balls were cleaned ultrasonically in petroleum ether and thoroughly air-dried.

RESULTS AND DISCUSSION

Synthesis and Spectroscopic Characterization. Three alkylborate-dithiophosphates with different alkyl chain lengths were synthesized following several steps (Scheme 1). The first step was followed by a procedure already reported for compounds with short alkyl chains:⁴³ Phosphorus pentasulfide (P₂S₅) was reacted with primary pentanol in a 1:4 molar ratio giving rise to *O,O'*-di-*n*-alkyldithiophosphoric acids. No further attempts were made to isolate and purify this acid because it tends to be slowly oxidized by atmospheric oxygen. Instead, the crude product was directly used to prepare three different potassium

O,O'-di-*n*-alkyldithiophosphate salts, which are more stable at ambient conditions. In the second step, *S*-hydroxyethyl of *O,O'*-di-*n*-alkyldithiophosphates were prepared by refluxing 2-chloroethanol with an aqueous suspension of potassium *O,O'*-di-*n*-alkyldithiophosphate salts in a 1:1 molar ratio for 3 h. In the third step, *S*-(di-*n*-alkylborate)-hydroxyethyl-*O,O'*-di-*n*-alkyldithiophosphates were obtained by treating *S*-hydroxyethyl of *O,O'*-di-*n*-alkyldithiophosphates with boric acid and a corresponding alcohol. The ethyl linker between sulfur and boron was introduced in these compounds in order to avoid a spontaneous decomposition, because direct boron–sulfur bonds are susceptible to hydrolysis by atmospheric moisture.

Both identity and purity of the products were checked by FT-IR and ¹H, ¹³C, ³¹P, and ¹¹B NMR spectroscopic measurements. The combined spectroscopic data were consistent with the structures of the intermediate and final compounds.

All characteristic bands in FTIR spectra of the intermediates and the final products were assigned (see Experimental Section and Figure SI-23 in the Supporting Information). The absorption frequencies of the aliphatic C–H vibrations in the alkyl groups of these compounds were mainly observed in the range 2957–2857 cm⁻¹. The medium and broad bands present in the FTIR spectra of all these three compounds in the region 984–980 cm⁻¹ were assigned to *ν*(P–OC), whereas bands in the region 730–708 and 666–540 cm⁻¹ were attributed to *ν*(P–S) and *ν*(P=S), respectively. However, it is difficult to distinguish with confidence between the P–S and P=S stretching frequencies. For example, vibration bands associated with the P–S stretching frequencies in the transition-metal complexes, which contain bidentate chelating dithiophosphate ligands, appear in the same region as for the free acids (RO)₂P(=S)SH and their thioesters (RO)₂P(=S)SR'.⁴⁴ There seems to be no significant shifts in stretching frequencies of P=S for the final products compared with the corresponding frequencies for their salts in the first step. This suggests a monodentate character of the thiophosphoryl group in all these compounds. For bidentate complexes this band is shifted to lower vibration frequencies compared with corresponding

salts of dithiophosphoric acids.⁴⁵ A strong and broad band around 3427 cm^{-1} , observed in *S*-hydroxyethyl of *O,O'*-di-*n*-alkyldithiophosphates only, is assigned here to $\nu(\text{O}-\text{H})$. In the final products, *S*-(di-*n*-alkylborate)-hydroxyethyl-*O,O'*-di-*n*-alkyldithiophosphates, a strong band around 1337 cm^{-1} is attributed to $\nu(\text{B}-\text{O})$. Obviously, it is absent in the intermediate products.

In the ^1H NMR spectrum of 100 mM solution of these compounds in CDCl_3 , multiplets at ca. 4.1 ppm are assigned to protons in CH_2OP molecular moieties. Apart from large deshielding typical for this group, and $^3J_{\text{HH}}$ -coupling with a neighbor CH_2 group, resonance lines are additionally split into a doublet by heteronuclear $^3J_{\text{HP}}$ -coupling between CH_2 protons and ^{31}P nucleus (spin $1/2$, 100% natural abundance). Similarly, a doublet of triplets at ca. 3 ppm is assigned to protons in the $\text{CH}_2-\text{S}-\text{P}$ fragment of alkylborate-dithiophosphates. Protons are J -coupled with phosphorus through a sulfur atom ($^3J_{\text{HP}} = 16.37\text{ Hz}$). Interestingly, no three-bond J -couplings were observed between CH_2 protons and boron in the borate part of these molecules (triplets at 3.76 and 3.96 ppm). ^{10}B and ^{11}B (spin $>1/2$) have a large quadrupolar moment and an asymmetric electric field gradient in the BO_3 fragment of the molecule, making $^3J_{\text{HB}}$ -coupling difficult to observe in isotropic liquids. Assignment of multiplets in the range of chemical shifts between 0.8 and 1.7 ppm to protons in different alkyl groups of alkylborate-dithiophosphate is rather straightforward using isotropic chemical shifts, J -couplings and integrals of the multiplets.

The chemical shift of phosphorus nucleus of potassium *O,O'*-di-*n*-alkyldithiophosphates in ethanol are around 112 ppm, while $\delta(^{31}\text{P})$ of *S*-hydroxyethyl of *O,O'*-di-*n*-alkyldithiophosphates in CDCl_3 are ca. 96 ppm. The 15 ppm upfield shift indicates the formation of a covalent $\text{P}-\text{S}-\text{C}$ bond in *S*-hydroxyethyl of *O,O'*-di-*n*-alkyldithiophosphates compared to the originally ionic fragment $\text{P}-\text{S}^-\text{K}^+$.⁴⁶ The ^{31}P NMR spectra of 100 mM *S*-(di-*n*-alkylborate)-hydroxyethyl-*O,O'*-di-*n*-alkyldithiophosphates in CDCl_3 reveal singlets around 96 ppm. The phosphorus sites in the final products are more shielded (by ca. 0.3 ppm) compared to P in the intermediates, *S*-hydroxyethyl of *O,O'*-di-*n*-alkyldithiophosphates, because of an additional alkyl borate group in *S*-(di-*n*-alkylborate)-hydroxyethyl-*O,O'*-di-*n*-alkyldithiophosphates covalently bound to P via the $-\text{S}-\text{CH}_2-\text{CH}_2-$ molecular moiety. Thus, ^{31}P NMR data additionally supports the completion of the reaction shown in Scheme 1 with the formation of intermediates and then the final products.

The ^{11}B NMR spectrum of the final products, *S*-(di-*n*-alkylborate)-hydroxyethyl-*O,O'*-di-*n*-alkyldithiophosphates, measured in CDCl_3 reveals singlets around 17.5 ppm, which suggests that the boron atom is coordinated to three oxygen atoms in the alkylborate groups.⁴⁷

Thermal Analyses. For lubricant additives used in mechanical systems at elevated temperatures, it is important to study the effect of temperature on their physicochemical properties, such as thermal stability, weight loss, and the nature of compounds formed during thermal decomposition. Two types of decomposition products were detected during the thermal decomposition of alkylborate-dithiophosphates in argon atmosphere: solid residues (with melting points above 500°C) and volatile products of pyrolysis of the alkyl and dithioalkyl groups (below 500°C). The volatile products were analyzed by quadrupole mass spectrometry (QMS). Small amounts of solid residues (ca. a few mg) formed from 200 mg of the liquid samples were not enough for the analysis using spectroscopic techniques such as

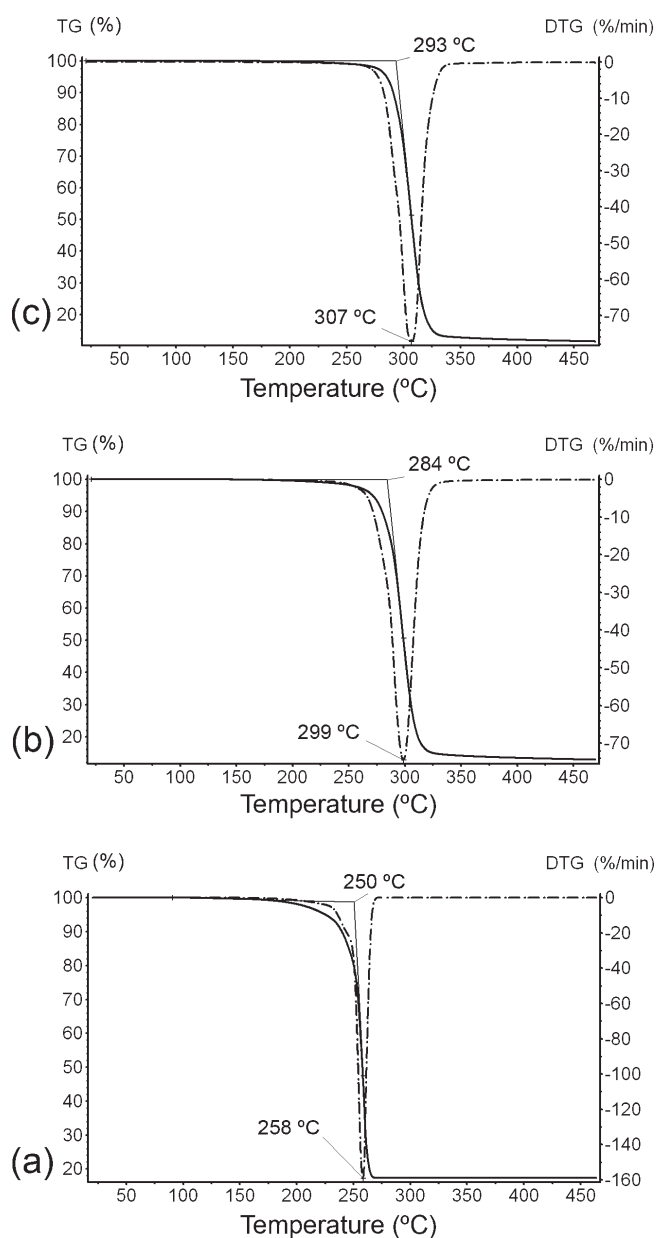


Figure 1. TG/DTG curves of (a) DPB-EDTP, (b) DOB-EDTP, and (c) DDB-EDTP at a heating rate of $20^\circ\text{C}/\text{min}$ and argon flow rate of $100\text{ mL}/\text{min}$.

FT-IR and/or solid-state NMR. To get enough amount of the residue for solid-state NMR spectroscopy, ca. 400 mg of DPB-EDTP was used in thermal analyses. The residual decomposition products of DPB-EDTP after TGA fall into two categories: (i) one product, which came out of the sample crucible and precipitated in the chamber, was a white jelly like material. (ii) The other decomposition product, which remained in the sample crucible, was a black powder material. After the thermal decomposition of DPB-EDTP, 75 mg of the white and 6 mg of the black products were collected from the instrument. Both the “white jelly-like” and the “black solid” materials were characterized by solid-state ^{13}C , ^{31}P , and ^{11}B NMR spectroscopy.

Thermogravimetric/derivative thermogravimetric (TG/DTG) curves indicate that these alkylborate-dithiophosphates exhibit a high thermal stability in a wide temperature range of up to

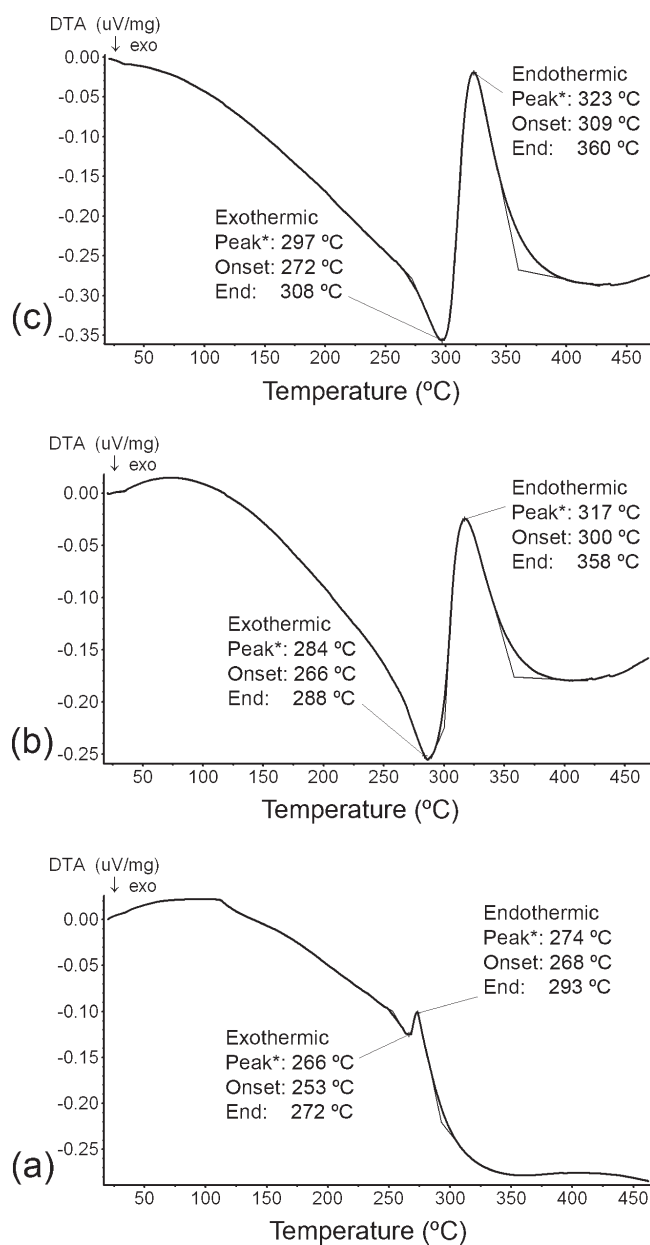


Figure 2. DTA curves for (a) DPB-EDTP, (b) DOB-EDTP, and (c) DDB-EDTP at a heating rate of 20 °C/min and argon flow rate of 100 mL/min.

250 °C (Figure 1). The TG curves show weight losses during the thermal decomposition of the compounds. Thermal decomposition of these compounds involves only one major step that occurs at 250, 284, and 293 °C for DPB-EDTP (Figure 1a), DOB-EDTP (Figure 1b), and DDB-EDTP (Figure 1c), respectively. The total weight loss during these tests was 83, 87, and 89 wt % for DPB-EDTP, DOB-EDTP and DDB-EDTP, respectively. The DTG curves show a weight loss per minute with an increase in temperature. For example, the rate of the weight loss for DPB-EDTP is just a few percent per min in the temperature interval 150–230 °C. It then increases dramatically and at 258 °C reaches its maximum value of 160% of the total weight of the sample per min. Similarly, the highest rate of the weight loss during the tests (at 299 °C for DOB-EDTP and 307 °C for DDB-EDTP) taken from DTG curves in Figure 1 is 74%/min for

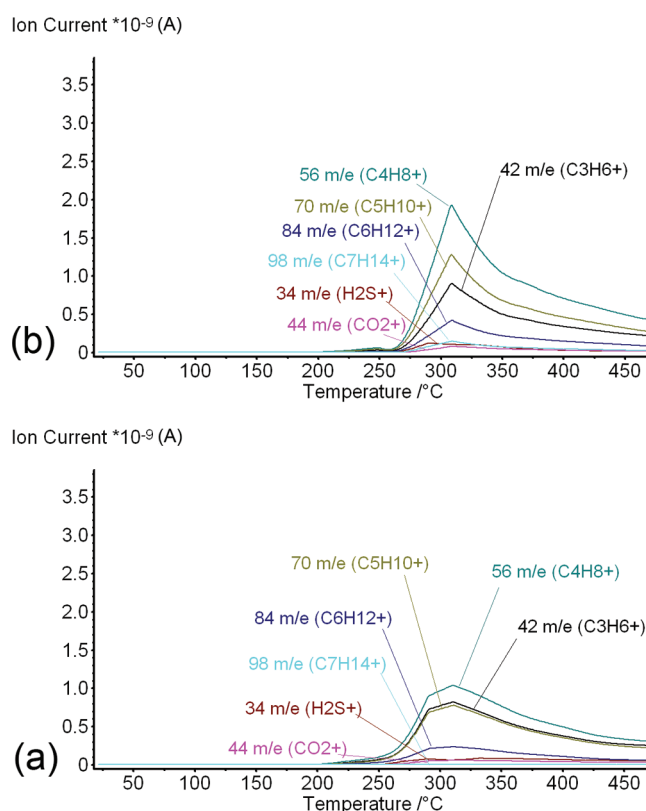


Figure 3. QMS profiles of (a) DOB-EDTP and (b) DDB-EDTP at a heating rate of 20 °C/min and argon flow rate of 100 mL/min: even molecular weight hydrocarbon fragments.

DOB-EDTP and 77%/min for DDB-EDTP. The thermal stability of these compounds increases with increasing length of the alkyl chains as DPB-EDTP < DOB-EDTP < DDB-EDTP.

The differential thermal analysis (DTA) curves of alkylborate-dithiophosphates are shown in Figure 2. Exothermic peaks are observed at 266, 284, and 297 °C for DPB-EDTP, DOB-EDTP, and DDB-EDTP, respectively. The exothermic peaks are followed by endothermic ones at 274 °C for DPB-EDTP, 317 °C for DOB-EDTP and 323 °C for DDB-EDTP, respectively. The former exothermic peaks represent the thermal decomposition, while the latter endothermic peaks represent the physical processes of the decomposed products such as melting, boiling, or other phase transitions.⁴⁸ Comparing Figures 1 and 2, one can notice that the exothermic peak is accompanied by a considerable weight loss of the sample due to the decomposition of the compound as has also been observed for other systems.⁴⁹

It is known that the main volatile decomposition products of dialkylidithiophosphates are hydrogen sulfide and olefins.⁵⁰ Therefore, the decomposition of the parent DOB-EDTP and DDB-EDTP compounds and the formation of volatile products as a function of temperature under a constant flow of argon gas were also analyzed by quadrupole mass spectrometry (QMS). A number of volatile products are formed and evolved in the temperature range from 20 to 500 °C. Evolution curves for some selected products formed in the course of the thermal decomposition of DOB-EDTP and DDB-EDTP are shown in Figure 3. The formation of hydrogen sulfide (H_2S^+) with $m/e = 34$ is observed during pyrolysis of both DOB-EDTP and DDB-EDTP. Olefins with various numbers of carbon atoms are formed under

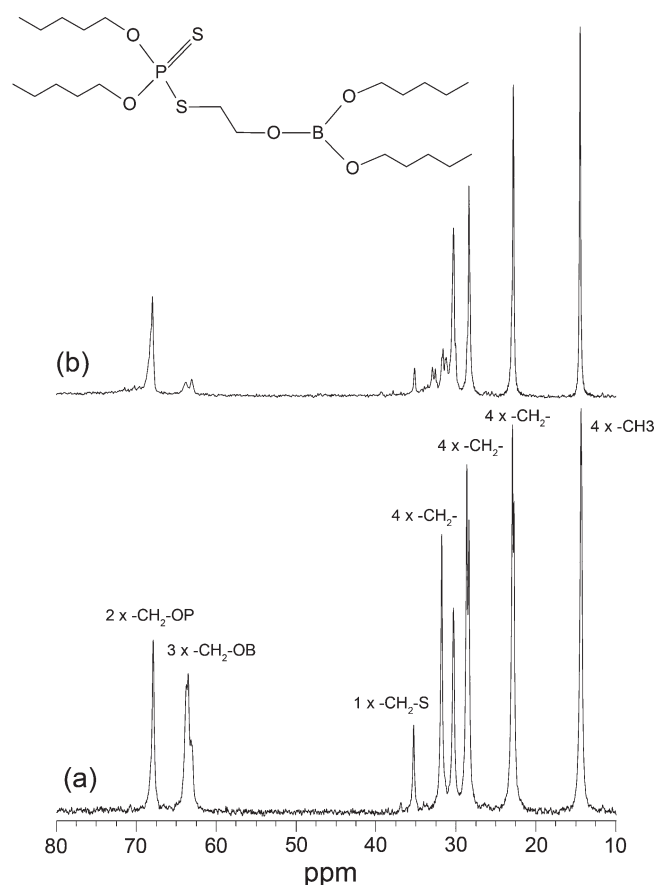


Figure 4. Single-pulse (CW proton decoupled) ^{13}C NMR spectra of (a) liquid DPB-EDTP with corresponding assignment of resonance lines and (b) the “white” jelly like residue of DPB-EDTP after its thermal decomposition in the course of DTA under argon atmosphere. The MAS frequency in b was 4.3 kHz; 512 and 5864 signal transients were accumulated in a and b, respectively. Inset represents the molecular structure of DPB-EDTP.

pyrolysis of parent alkyl chains in the boron compounds studied. Relative intensities of hydrocarbon fragments in comparison with H_2S^+ are plotted for both parent compounds (see Figure 3). The propenyl cation (C_3H_6^+ with $m/e = 42$), butenyl cation (C_4H_8^+ with $m/e = 56$) and pentenyl cation ($\text{C}_5\text{H}_{10}^+$ with $m/e = 70$) have rather similar evolution patterns. They are the principle components in the mixture of volatile products of decomposition of these compounds. Olefin cations with larger molecular weights ($\text{C}_6\text{H}_{12}^+$ and $\text{C}_7\text{H}_{14}^+$) have smaller intensities in the QMS profiles as compared to cations with three, four, and five carbon atoms in the chain.

The novel compounds studied here are more thermally stable compared to *S*-di-*n*-octoxyboron-*O*,*O'*-di-*n*-octyldithiophosphate, DOB-DTP, in which boron is directly bonded to the sulfur atom of dialkyldithiophosphate.³⁵ The thermal behavior of that compound was analyzed using the same experimental conditions as in the current study. Interestingly, the pyrolysis of alkyl chains in DOB-EDTP and DDB-EDTP takes place before the formation of H_2S^+ . However, during decomposition of DOB-DTP, H_2S^+ is formed before pyrolysis of alkyl chains.³⁵ This suggests that the B–S bond in DOB-DTP is thermally less stable than C–S or B–O bonds in DOB-EDTP and DDB-EDTP compounds.

NMR on Residues of DPB-EDTP after Thermal Analyses. A combined solid-state multinuclear, ^{13}C , ^{31}P , and ^{11}B MAS NMR

was used for monitoring the physicochemical changes, which occurred after the thermal decomposition of DPB-EDTP and for characterizing amorphous and/or crystalline residues of this compound after TGA. Proton-decoupled ^{13}C NMR spectra of both liquid DPB-EDTP before and the “white” jelly like residue of DPB-EDTP after TGA are shown in Figure 4. The complete assignment of ^{13}C chemical shifts of DPB-EDTP is given in the Experimental Section. By comparing ^{13}C NMR resonance lines in the range of 10 to 40 ppm assigned to aliphatic carbon atoms one can notice that the spectrum of the “white” residue of DPB-EDTP after TGA (Figure 4b) reveals a smaller number of resonance lines in this spectral interval compared to the spectrum of DPB-EDTP before TGA (Figure 4a). This suggests that some alkyl groups are cleaved out in the course of thermal decomposition of DPB-EDTP. However, the most noticeable changes are visible between 60 and 70 ppm in ^{13}C NMR spectra of these compounds. In DPB-EDTP three resonance lines around 63–64 ppm were assigned to three nonequivalent carbon atoms in $-\text{CH}_2-\text{O}-$ groups bound to the boron, whereas the single resonance line at 68 ppm was attributed to two carbon atoms in $-\text{CH}_2-\text{O}-$ groups bound to phosphorus, i.e., in the dialkyldithiophosphate group of the DPB-EDTP molecule. In the single-pulse ^{13}C MAS NMR spectrum of the “white” residue of DPB-EDTP after TGA ^{13}C resonance lines assigned to carbons in the $(-\text{CH}_2\text{O})_3\text{B}$ molecular moiety have almost vanished (see Figure 4b). This confirms that the $(-\text{CH}_2\text{O})_3\text{B}$ group is cleaved from DPB-EDTP during the thermal analysis and derivatives of dialkyldithiophosphates (but not of the trialkylborate group) are present in the “white” residue of DPB-EDTP. A $^1\text{H}-^{13}\text{C}$ cross-polarization MAS NMR experiment was also performed on the “white” residue of DPB-EDTP. A ^{13}C CP/MAS NMR spectrum of the latter sample (not shown here, see Figure SI-9 in the Supporting Information) is almost identical to the single-pulse ^{13}C MAS NMR spectrum presented in Figure 4b. Since species in the “white” jelly like residue of DPB-EDTP are detected in the ^{13}C CP/MAS NMR experiment, these molecules lack a rotational mobility and, thus, they are most probably adsorbed to surfaces of small solid particles of borophosphates, which are also present in the same sample as was elucidated by both ^{13}P and ^{11}B NMR and further discussed in detail below. As expected, borophosphates composed of boron, phosphorus and oxygen but lacking carbon atoms, were neither detected in the single-pulse MAS nor in CP/MAS ^{13}C NMR experiments discussed above. Thus, ^{13}C NMR data suggest that the borate fragment of DPB-EDTP is cleaved before the decomposition of the dialkyldithiophosphate group of the molecule that takes place at high temperatures during TGA.

^{31}P NMR spectra of pure DPB-EDTP and the “white” jelly-like product of it after TGA under argon atmosphere are shown in Figure 5. The ^{31}P NMR spectrum of pure DPB-EDTP reveals a single ^{31}P resonance line at 95.9 ppm (Figure 5a). After the thermogravimetric analysis of DPB-EDTP, ^{31}P NMR spectrum of the collected white residual of this compound shows several additional resonance lines in the range from 96 to –30 ppm: The ^{31}P NMR resonance lines at ca. 68 ppm are here assigned to trialkylmonothiophosphates, $(\text{RO})_3\text{P}=\text{S}$, these at ca. 28 ppm to *S*-alkyl-*O*,*O*-dialkylphosphates, $\text{O}=\text{P}(\text{OR})_2\text{SR}$,⁵¹ and resonance peaks at ca. –1 ppm can be assigned to phosphorus sites in either dialkylphosphoric acid, $\text{O}=\text{P}(\text{OR})_2\text{OH}$, or trialkylphosphates, $\text{O}=\text{P}(\text{OR})_3$.⁵² In addition, broad ^{31}P NMR signals (see also an insert of Figure 5b with an expanded region of this spectrum) were observed at ca. –14, –22, and –30 ppm and can

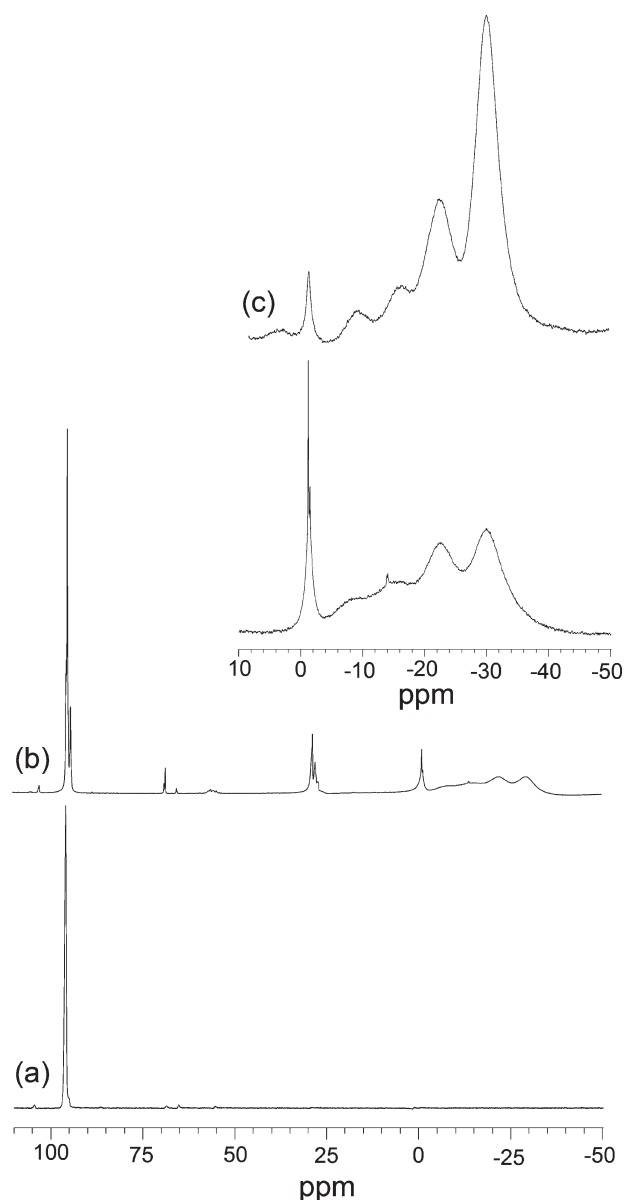


Figure 5. Single-pulse ^{31}P NMR spectra of (a) liquid DPB-EDTP, (b) the “white” jelly like residual, and (c) the black residual after a thermal decomposition of DPB-EDTP under argon atmosphere. The MAS frequency was 10.0 kHz in b and 5.0 kHz in c; 128 and 3055 signal transients were accumulated in a and b, respectively. The expanded region of ^{31}P NMR spectrum b between 10 and -50 ppm is shown in the inset.

be assigned to traces of solid inorganic polyphosphates present in the same sample.⁵³ Therefore, a number of different decomposition products were formed as a result of cleavage of different bonds, intermolecular rearrangements and oxidation of $\text{P}=\text{S}$ to $\text{P}=\text{O}$ bonds in the course of heating of DPB-EDTP in the argon atmosphere.

^{31}P MAS spectrum of the “black” residue of DPB-EDTP after its thermal decomposition under argon atmosphere is shown in Figure 5c. The single-pulse ^{31}P MAS spectrum of this residue reveals, along with a sharp resonance line at ca. 0 ppm assigned to orthophosphates, other broad resonance lines at 0.3, -8.0 , -14.8 , -21.5 , and -29.5 ppm (see Figure 5c and

Table 1. ^{31}P NMR Parameters Obtained from Deconvoluted Single-Pulse ^{31}P MAS NMR Spectra of Residues of DPB-EDTP after TGA

^{31}P chemical shift (ppm)	line width (ppm)	relative integral intensity
“White” Residue		
-1.2	0.2	0.01
-1.4	1.3	0.08
-8.1	6.8	0.08
-14.0	0.5	0.002
-15.6	8.4	0.20
-22.5	4.9	0.21
-30.2	7.4	0.42
“Black” Residue		
0.3	1.1	0.03
-8.0	3.7	0.04
-14.8	5.8	0.11
-21.5	4.9	0.25
-29.5	4.6	0.57

Table 1). -29.5 ppm is the characteristic chemical shift of phosphorus sites in amorphous BPO_4 glasses that has previously been assigned to ^{31}P in phosphate anions tetrahedrally coordinated by four boron atoms through $\text{P}-\text{O}-\text{B}$ bonds.^{54,55} The resonance lines at -21.5 , -14.8 , and -8.0 ppm can be assigned to either polyphosphates or aluminum phosphates formed in reactions between DPB-EDTP and the alumina (Al_2O_3) that the sample crucible was made of.⁵⁶ A $^{31}\text{P}\{^1\text{H}\}$ CP/MAS NMR spectrum of the “black” residue of DPB-EDTP (see Figure SI-12 in the Supporting Information) amplifies resonance lines from phosphorus sites, which are in a close vicinity to protons from surface OH groups or surface adsorbed water molecules (the dominant resonance peak at -21.5 ppm). However, the resonance line at -29.5 ppm has a considerably smaller relative integral intensity in the ^{31}P CP/MAS compared with the single-pulse ^{31}P MAS NMR spectrum of the same compound that additionally supports the assignment of this resonance line to phosphorus sites in amorphous BPO_4 without protons in the bulk of this phase.

Results of deconvolution of the single-pulse ^{31}P NMR spectra of both the “white” and the “black” residues of DPB-EDTP after TGA, i.e. resonance peak positions, line-widths and relative integral intensities corresponding to phosphorus sites in different products of the thermal decomposition of DPB-EDTP, are summarized in Table 1. Representative examples of the peak fits for these products are shown in the Supporting Information (see Figures SI-10 and SI-11).

Figure 6 shows a ^{11}B single-pulse NMR spectrum of liquid DPB-EDTP (Figure 6a) and ^{11}B single-pulse MAS NMR spectra of both “white” (Figure 6b) and “black” (Figure 6c) residues of DPB-EDTP after TGA. The ^{11}B NMR spectrum of pure DPB-EDTP before TGA reveals a single resonance line at 17.6 ppm, which is assigned to the three-coordinated alkylborate group in liquid DPB-EDTP. This resonance line is not present in ^{11}B NMR spectra of the decomposed products of DPB-EDTP, which directly confirms the conclusions from both ^{13}C and ^{31}P NMR that the alkylborate part of this molecule is cleaved out during the thermal decomposition of DPB-EDTP. ^{11}B MAS NMR spectra of the residues of DPB-EDTP reveal a single resonance line at ca -3.3 ppm signifying four-coordinated boron units ($\text{B}^{(4)}$) in

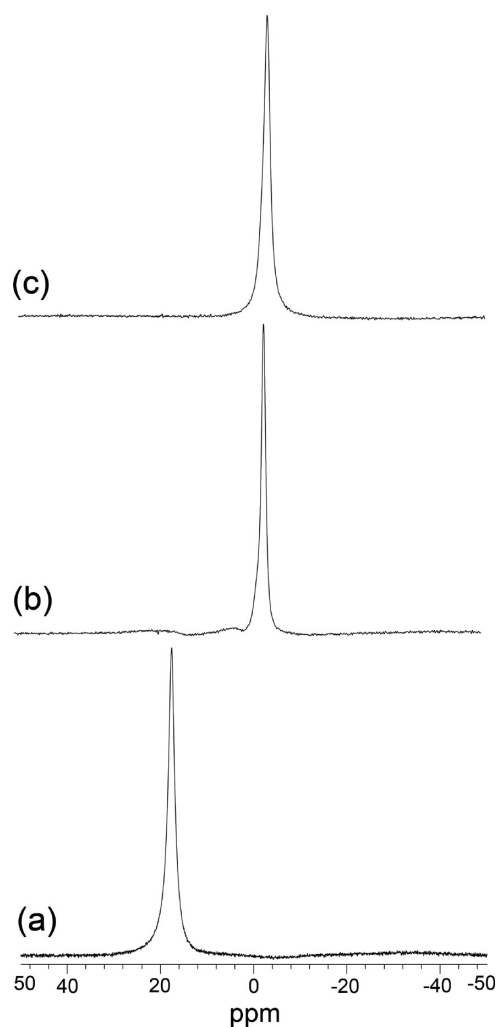


Figure 6. (a) Single-pulse ^{11}B NMR spectrum of liquid DPB-EDTP and single-pulse ^{11}B MAS NMR spectra of (b) the “white” and (c) “black” residues of DPB-EDTP after TGA. The MAS frequency was 10 kHz in both b and c. Total of 16 (in a) and 216 (in b and c) signal transients were accumulated.

these compounds.⁵⁷ The ^{11}B NMR signal at -3.3 ppm has previously been assigned to the $\text{B}^{(4)}$ groups linked to three ($\text{B}^{(4)}_{3\text{P}}$) or four ($\text{B}^{(4)}_{4\text{P}}$) phosphorus atoms in the glass with composition $(\text{Na}_2\text{O})_{0.4}[(\text{B}_2\text{O}_3)_{0.4}(\text{P}_2\text{O}_5)_{0.6}]_{0.6}$.⁵⁸ Therefore, our ^{31}P and ^{11}B NMR data suggest that borophosphate compounds are present in both the “white” and the “black” products of decomposition of DPB-EDTP after TGA. In addition, the single sharp and symmetrical ^{11}B NMR resonance line in these spectra also suggests that only one type of boron sites ($\text{B}^{(4)}$) is present in these borophosphates (with only small traces of other boron-containing compounds present in the “white” residue of DPB-EDTP, see Figure 6b).

It has been previously reported that tribofilms formed by lubricants with ZnDTP/calcium borate additives contain borophosphates.⁵⁹ The tribofilms containing borophosphates provide a lower coefficient of friction compared to tribofilms containing polyphosphates formed by lubricants with ZnDTP. Therefore, the formation of borophosphates at the interfaces is an additional advantage of boron-dithiophosphate compounds over ZnDTPs and other ashless phosphorus and sulfur containing lubricant additives.

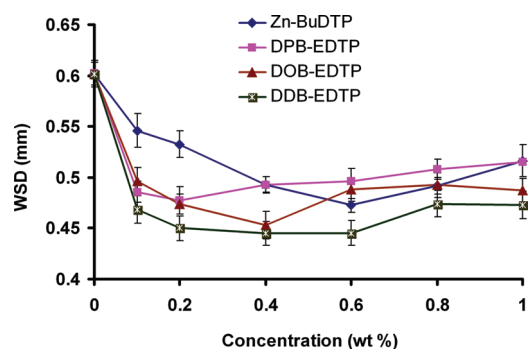


Figure 7. Mean WSD dependence on additives concentration in mineral oil of DPB-EDTP (squares), DOB-EDTP (triangles), DDB-EDTP (stars), and Zn-BuDTP (rhombs). Tests were performed in a four-ball tribometer at ambient temperature (294 K) and 392 N load during 30 min.

On the basis of the results from solid-state NMR on residues of DPB-EDTP after TGA we propose the following sequence of events in the pyrolysis of this compound: Cleavage of DPB-EDTP is initiated at temperatures above 200 °C, when the dialkyldithiophosphate group is separated from the alkylborate molecular moiety. Some amounts of these decomposed products came out from the sample crucible with a heat and gas flow, while some remained inside the crucible. The product that came out from the sample crucible was a jelly like white material, which is composed mainly of alkylidithiophosphates with some traces of solid particles of borophosphates. Decomposition of the product that remained inside the sample crucible proceeded further at higher temperatures. It resulted in the formation of the solid black inorganic material (no carbon atoms were detected in this sample by ^{13}C MAS NMR). The solid black material is formed as a result of cleavage of all alkyl groups and rearrangement of boron, oxygen and phosphorus atoms into a borophosphate phase at higher temperatures. Solid-state NMR data confirmed that this inorganic black material consists of borophosphates, traces of which are also present in the white jelly-like material. Hence, it is suggested that borophosphate films may also be formed by the DPB-EDTP additive adsorbed on boundary lubricated metal surfaces during sliding at high “flash” temperatures.

Tribological Performance. A commercially available ZnDTP contains a mixture of 85% *O,O'*-di-*iso*-butyl-dithiophosphato-zinc(II) and 15% *O,O'*-di-*n*-octyl-dithiophosphato-zinc(II).⁶⁰ In this study, we selected *O,O'*-di-*n*-butyl-dithiophosphato-zinc(II) (as a reference compound) with the same number of carbon atoms in alkyl chains as in the principal component of the commercial ZnDTP additive. We preferred Zn-BuDTP for tribological studies instead of solid *O,O'*-di-*iso*-butyl-dithiophosphato-zinc(II) because the former compound is a liquid at ambient temperatures with a high solubility in the mineral oil used in our studies. The antiwear and friction performance of these novel alkylborate-dithiophosphates and Zn-BuDTP was evaluated using the same base oil and test conditions. It is known that the concentration of additives in base oil plays an important role in both friction and wear performance. Therefore, tests were conducted in the concentration range from 0 to 1.0 wt % of either alkylborate-dithiophosphates or Zn-BuDTP. Figure 7 shows variations of the mean WSD of the lower steel balls lubricated with the base oil containing either alkylborate-dithiophosphates or Zn-BuDTP additives at different concentrations. All these

novel compounds and Zn-BuDTP are found to reduce WSDs when added to the base oil even at very small concentrations. A decrease in the WSD was detected up to some optimum concentrations of these alkylborate-dithiophosphate compounds in the base oil. Then WSD gradually increases with an increase of concentration of the additive. A similar trend was also found for Zn-BuDTP. The optimum concentrations for the wear reducing ability of an additive in the base oil in the steel–steel contacts were around 0.2 (3.26 mM) and 0.6 wt % (8.92 mM) for DPB-EDTP and Zn-BuDTP additives, respectively. At the optimum concentration, 0.2 wt % (3.26 mM) of DPB-EDTP, the amount of sulfur is 0.026 wt % (6.52 mM) and the amount phosphorus is 0.012 wt % (3.26 mM). Similarly, at the optimum concentration, 0.6 wt % (8.92 mM) of Zn-BuDTP, the amount of sulfur is 0.140 wt % (35.68 mM) and phosphorus is 0.068 wt % (17.84 mM). It reveals that for antiwear performance under the tribological conditions studied, the optimum concentrations of sulfur and phosphorus are 5.5 times lower in case of DPB-EDTP compared with Zn-BuDTP.

Similarly, the WSDs for 0.4 wt % of DOB-EDTP (4.87 mM) and DDB-EDTP (4.17 mM) decrease reaching minimum values of 0.45 mm for the former and 0.44 mm for the latter compound. It is evident that the antiwear performance of DDB-EDTP is superior compared to the other compounds at all concentrations studied (0.1–1.0 wt %). In particular, the WSD for DDB-EDTP is the smallest (<0.45 mm) at a wider range of concentrations (0.2–0.6 wt %).

In this regard, a pertinent question is: Why is the optimum concentration for alkylborate-dithiophosphates lower than that of Zn-BuDTP?

First of all, it is known that the increase in WSD at higher concentrations of additives (observed for all compounds) is due to a corrosive action of sulfur present in these compounds. There might be at least two reasons for remarkably different antiwear behavior of alkylborate-dithiophosphates compared to Zn-BuDTP. First, we anticipate that sulfur and phosphorus atoms present in alkylborate-dithiophosphates are more reactive than P and S in Zn-BuDTP. Thus, even a very small concentration of alkylborate-dithiophosphates is sufficient for formation of protective tribofilms on steel surfaces. Second, alkylborate-dithiophosphates contain an alkyl borate group that may additionally enhance the antiwear ability of this additive and inhibit a part of the corrosive action of sulfur even at high concentrations of alkylborate-dithiophosphates in the base oil.

Figure 8 shows variations of the friction coefficient with concentration (wt %) for these additives in the base oil under study. Incorporation of Zn-BuDTP in the base oil does increase significantly (by more than 50%) the friction coefficient of the resulting lubricant. In contrast, the friction coefficient of the lubricant with 0.1–0.6 wt % DPB-EDTP does not increase. The friction coefficient for the base oil with DOB-EDTP or DDB-EDTP does increase by ca. 25–35%, i.e., at a smaller extent as compared with an increase of the friction coefficient for the base oil with Zn-BuDTP. What could be even more attractive for future tribological applications is the fact that the friction coefficient of the lubricant with DPB-EDTP does not increase with an increase in concentration up to 0.6 wt % of the novel additive, whereas the friction coefficient increases considerably for the base oil with Zn-BuDTP in the whole concentration range studied compared to the friction coefficient for the base oil only.

It is already known that the tribofilms formed by ZnDTPs⁶¹ and S-di-*n*-octoxyboron-*O,O'*-di-*n*-octyldithiophosphate (DOB-

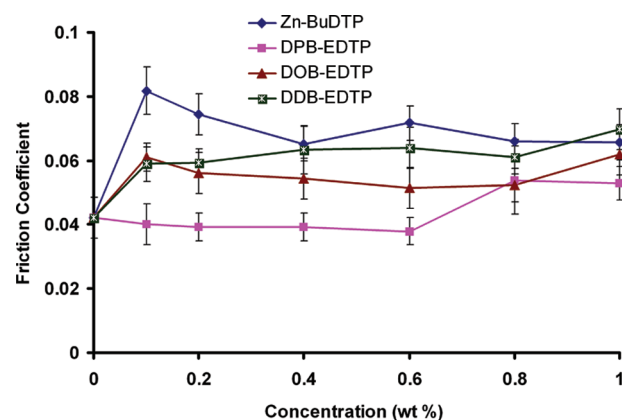


Figure 8. Friction coefficient (an average over last 10 min) as a function of additives concentration in the mineral oil for DPB-EDTP (squares), DOB-EDTP (triangles), DDB-EDTP (stars) and Zn-BuDTP (rhombs). Tests were performed in a four-ball tribometer at ambient temperature (294 K) and 392 N load during 30 min.

DTP)³⁵ cause an increase in the friction coefficient. However, a mechanism of a significant increase in the coefficient of friction for lubricants with these additives has not yet been fully explained. Tribofilms formed from DPB-EDTP seem to have considerably lower shear strength and weaker interfacial bonds compared to both Zn-BuDTP and DOB-DTP.

It is known that during a sliding process low energy electrons are emitted from the contact point at the metal surface. This results in the formation of positive charge at the surface.⁶² At the same time, the discussed alkylborate dithiophosphate compounds break down into fragments containing iron reactive elements such as phosphorus, sulfur and boron. Recently, Tse⁶³ and Oganov et al.⁶⁴ have found that elemental boron has partially negative charge under pressure. The negatively charged molecular fragments of alkylborate-dithiophosphates such as mono- and dithiophosphate anions, borophosphate anions and borate anions can be easily adsorbed onto the positively charged metal surfaces because of the electrostatic interaction. Finally, phosphate, borophosphate and borate based tribofilms can be formed on the steel surfaces in boundary lubrication conditions. The tribofilms formed by alkylborate-dithiophosphates provide lower and more stable friction over a wide range of concentrations of the additive (0.1–0.6 wt %) that is important for the durability and a better functionality of mechanical systems.

Surface Analysis. After tribological tests, the wear scars were analyzed using scanning electron microscopy/energy-dispersive X-ray spectroscopy (SEM/EDS) techniques (Figures 9 and 10). The worn surfaces of balls lubricated with the base oil containing alkylborate-dithiophosphate and Zn-BuDTP additives were studied by this technique to compare both morphology and composition of the tribofilms formed. SEM/EDS data obtained suggests the formation of tribofilms containing both sulfur and phosphorus depending on the type of additive and its concentration.

Figure 9 shows a SEM micrograph of the worn surface lubricated by the base oil without additives and oil containing additives. The micrograph of the ball lubricated with the base oil only clearly shows wide grooves, indicating significant wear (see Figure 9a). Figures 9b–d show worn surfaces lubricated by the base oil with 1.0 wt % of Zn-BuDTP (Figure 9b), DOB-EDTP (Figure 9c) and DDB-EDTP (Figure 9d). These images suggest that tribofilms formed on steel surfaces lubricated by the mineral

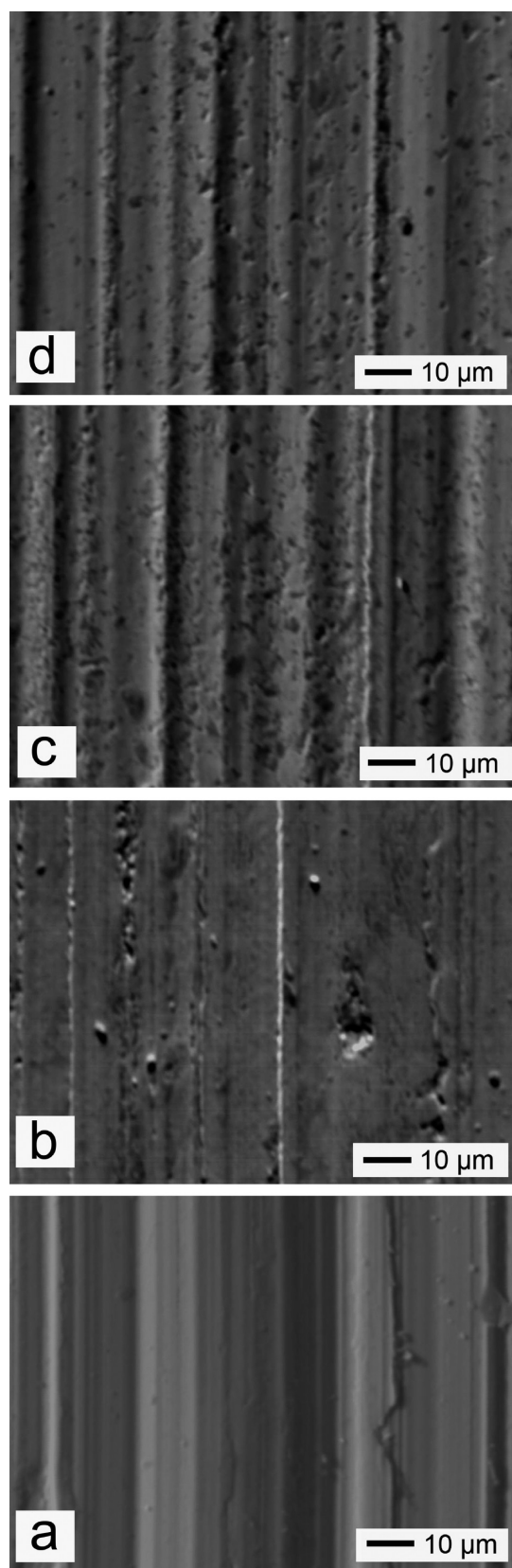


Figure 9. SEM micrographs of worn ball surfaces lubricated with (a) base oil; (b) base oil containing 1.0 wt % of Zn-BuDTP; (c) DOB-EDTP; (d) DDB-EDTP.

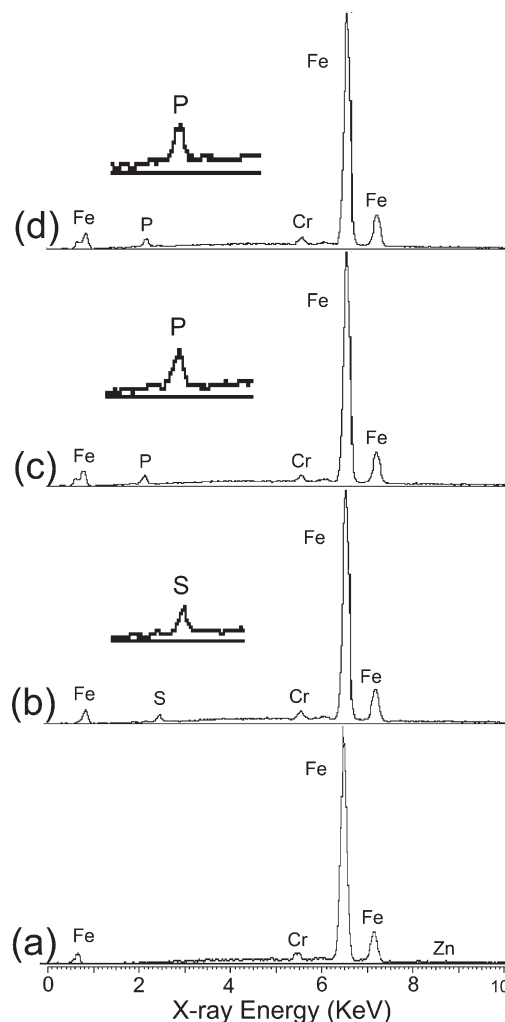


Figure 10. EDS spectra of tribofilms formed worn ball surfaces lubricated with (a) base oil and (b) base oil containing 1.0 wt % of Zn-BuDTP; (c) DOB-EDTP; (d) DDB-EDTP. The EDS spectra are the average of the area shown in the corresponding micrographs in Figure 9.

oil with boron-based additives have a different morphology compared to tribofilms in the lubricant with Zn-BuDTP.

A corresponding EDS analysis suggests a transfer/adsorption of active elements from the additives to the steel surfaces. Figure 10 clearly shows depositions of sulfur from Zn-BuDTP and phosphorus from DOB-EDTP and DDB-EDTP on the worn surfaces. Boron was not detected on the worn surfaces lubricated by the base oil containing DOB-EDTP or DDB-EDTP, because of a low sensitivity of the EDS method to light elements. Interestingly, phosphorus was the predominant element in depositions from either DOB-EDTP or DDB-EDTP (maybe in the form of borophosphate glasses), while sulfur dominated in the surface layers formed by products of decomposition of Zn-BuDTP.

CONCLUSION

Novel zinc-free compounds, alkylborate-dithiophosphates, with a low content of sulfur and phosphorus are designed as additives for lubricants. Their interfacial performance in steel-to-steel contacts in a mineral oil was studied in terms of friction and antiwear characteristics. The thermal behavior of these compounds was studied by TG/DTG, DTA, and QMS analyses. All these

compounds showed a high thermal stability and a good miscibility with the mineral oil. The thermal stability of these alkylborate-dithiophosphates increased with increasing the length of alkyl chains. Solid-state NMR data suggested the decomposition of DPB-EDTP into different phosphate species and revealed the formation of borophosphates as final products of these thermally induced reactions.

Alkylborate-dithiophosphates significantly reduce wear of the steel surfaces. DDB-EDTP provides the lowest wear rates compared to DPB-EDTP, DOB-EDTP and Zn-BuDTP in the concentration range 0.1–1.0 wt %. Tribofilms, formed on the steel surfaces when the novel additives are admixed in the mineral oil, enhance steel-to-steel contact performance. All alkylborate-dithiophosphates studied, show lower friction coefficients compared to Zn-BuDTP in the concentration range 0.1–1.0 wt %. The friction coefficient remained low and stable (≤ 0.04) up to concentration of DPB-EDTP 0.6 wt %. Therefore, these novel alkylborate-dithiophosphate compounds can be considered as efficient environmentally friendly replacement of ZnDTPs.

■ ASSOCIATED CONTENT

S Supporting Information. ^1H , ^{13}C , ^{31}P , and ^{11}B NMR spectra of reaction intermediates, final compounds of alkylborate-dithiophosphates, and residues of DPB-EDTP after thermal analyses, table of numerical values for antiwear and friction performance, optical profiles, SEM/EDS for wear scars. This material is available free of charge via the Internet at <http://pubs.acs.org>.

■ AUTHOR INFORMATION

Corresponding Author

*E-mail: Oleg.Antzutkin@ltu.se (O.N.A.); segla@ltu.se (S.G.).

■ ACKNOWLEDGMENT

The financial support (a stipend for F.U.S.) provided by the Foundation in memory of J. C. and Seth M. Kempe is gratefully acknowledged. A Varian/Chemagnetics InfinityPlus CMX-360 spectrometer was purchased with a grant from the Swedish Council for Planning and Coordination of Research (FRN) and further upgraded with JCK-2003, JCK-2307 and JCK-2905 grants from the Foundation in memory of J. C. and Seth M. Kempe. Foundation in memory of J. C. and Seth M. Kempe is also acknowledged for a few grants for equipment at the Tribolab at Luleå University of Technology.

■ REFERENCES

- (1) Lara, J.; Blunt, T.; Kotvis, P.; Riga, A.; Tysoe, W. T. *J. Phys. Chem. B* **1998**, *102*, 1703–1709.
- (2) Bhushan, B.; Israelachvili, J. N.; Landman, U. *Nature* **1995**, *374*, 607–616.
- (3) Kotvis, P. V.; Huezo, L. A.; Tysoe, W. T. *Langmuir* **1993**, *9*, 467–474.
- (4) Didziulis, S. V. *Langmuir* **1995**, *11*, 917–930.
- (5) Gao, F.; Furlong, O.; Kotvis, P. V.; Tysoe, W. T. *Langmuir* **2004**, *20*, 7557–7568.
- (6) Mosey, N. J.; Woo, T. K. *J. Phys. Chem. A* **2003**, *107*, 5058–5070.
- (7) Willermet, P. A.; Carter, R. O.; Boulos, E. N. *Tribol. Int.* **1992**, *36*, 371–380.
- (8) Mosey, N. J.; Woo, T. K. *J. Phys. Chem. A* **2004**, *108*, 6001–6016.

- (9) Zhang, Z.; Najman, M.; Kasrai, M.; Bancroft, G. M.; Yamaguchi, E. S. *Tribol. Lett.* **2005**, *18*, 43–51.
- (10) Mosey, N. J.; Woo, T. K. *Inorg. Chem.* **2005**, *44*, 7274–7276.
- (11) Hsu, S. M.; Gates, R. S. *Tribol. Int.* **2005**, *38*, 305–312.
- (12) Hsu, S. M. *Langmuir* **1996**, *12*, 4482–4485.
- (13) Mosey, N. J.; Müser, M. H.; Woo, T. K. *Science* **2005**, *307*, 1612–1615.
- (14) Spikes, H. *Tribol. Lett.* **2004**, *17*, 469–489.
- (15) Nicholls, M. A.; Do, T.; Norton, P. R.; Kasrai, M.; Bancroft, G. M. *Tribol. Int.* **2005**, *38*, 15–39.
- (16) Fuller, M. L. S.; De Jong, K. L.; Kasrai, M.; Bancroft, G. M. *Chem. Mater.* **2000**, *12*, 1300–1304.
- (17) Piras, F. M.; Rossi, A.; Spencer, N. D. *Langmuir* **2002**, *18*, 6606–6613.
- (18) Onodera, T.; Morita, Y.; Suzuki, A.; Koyama, M.; Tsuboi, H.; Hatakeyama, N.; Endou, A.; Takaba, H.; Kubo, M.; Dassenoy, F.; Minfray, C.; Joly-Pottuz, L.; Martin, J. M.; Miyamoto, A. *J. Phys. Chem. B* **2009**, *113*, 16526–16536.
- (19) Isaksson, M.; Frick, M.; Gruvberger, B.; Ponten, A.; Bruze, M. *Contact Dermatitis* **2002**, *46*, 248–249.
- (20) Cisson, C. M.; Rausina, G. A. *Lubr. Sci.* **1996**, *8*, 145–177.
- (21) Spikes, H. *Lubr. Sci.* **2008**, *20*, 103–136.
- (22) Baldwin, B. A. *Wear* **1977**, *45*, 345–353.
- (23) Herdan, J. M. *Lubr. Sci.* **2000**, *12*, 265–276.
- (24) Varlota, K.; Kasrai, M.; Bancroft, G. M.; De Stasio, G.; Gilbert, B.; Yamaguchi, E. S.; Ryason, P. R. *Tribol. Lett.* **2003**, *14*, 157–166.
- (25) Martin, J. M.; Grossiord, C.; Varlot, K.; Vacher, B.; Igarashi, J. *Tribol. Lett.* **2000**, *8*, 193–201.
- (26) Stanulov, K. G.; Harhara, H. N.; Cholakov, G. S. *Tribol. Int.* **1998**, *31*, 257–263.
- (27) Zhang, J.; Liu, W.; Xue, Q. *Wear* **1999**, *224*, 68–72.
- (28) Sun, Y.; Hu, L.; Xue, Q. *Wear* **2009**, *266*, 917–924.
- (29) Wang, W.; Chen, K.; Zhang, Z. *J. Phys. Chem. C* **2009**, *113*, 2699–2703.
- (30) Ball, P. *Nat. Mater.* **2010**, *9*, 6–6.
- (31) Klepper, C. C.; Williams, J. M.; Truhan, J. J.; Qu, J.; Riester, L.; Hazelton, R. C.; Moschella, J. J.; Blau, P. J.; Anderson, J. P.; Popoola, O. O.; Keitz, M. D. *Thin Solid Films* **2008**, *516*, 3070–3080.
- (32) Latini, A.; Rau, J. V.; Teghil, R.; Generosi, A.; Albertini, V. R. *ACS Appl. Mater. Interfaces* **2010**, *2*, 581–587.
- (33) Chung, H. Y.; Weinberger, M. B.; Levine, J. B.; Kavner, A.; Yang, J. M.; Tolbert, S. H.; Kaner, R. B. *Science* **2007**, *316*, 436–439.
- (34) Martini, C.; Palombarini, G. *J. Mat. Sci.* **2004**, *39*, 933–937.
- (35) Shah, F. U.; Glavatskih, S.; Antzutkin, O. N. *ACS Appl. Mater. Interfaces* **2009**, *1* (12), 2835–2842.
- (36) Ivanov, A. V.; Antzutkin, O. N.; Larsson, A. C.; Kritikos, M.; Forsling, W. *Inorg. Chim. Acta* **2001**, *315*, 26–35.
- (37) Larsson, A. C.; Ivanov, A. V.; Forsling, W.; Antzutkin, O. N.; Abraham, A. E.; de Dios, A. J. *Am. Chem. Soc.* **2005**, *127* (7), 2218–2230.
- (38) Karaghiosoff, K. *Encyclopedia of Nuclear Magnetic Resonance*; Grant, D. M.; Harris, R. K., Eds.; Wiley: New York, 1996; Vol. 6, p 3612.
- (39) Komon, Z. J. A.; Rogers, J. S.; Bazan, G. C. *Organometallics* **2002**, *21*, 3189–3195.
- (40) Morcombe, C. R.; Zilm, K. W. *J. Magn. Reson.* **2003**, *162* (2), 479–486.
- (41) <http://www.mikrokemi.se>. The elemental analysis for C and H was performed according to Dumas method using Flash EA 1112 from Thermo Finnigan elemental analyser. About 1 mg of the sample was weighed in tin capsule, sealed and placed in an auto sampler, from which it was dropped into a combustion chamber. As the sample entered the combustion chamber oxygen was injected into the carrier gas (He), which flowed through the combustion tube. The temperature was raised to 1800 °C, which ensured the complete combustion of the sample. Detection was made with a Hot Wire Detector (HWD). The quantification was made using certified external standards and the method of least-squares with the correlation coefficient >0.999.
- (42) <http://www.analytica.se>. For B elemental analysis, approximately 50 mg of sample was digested with 1 mL concentrated HNO₃.

(micro wave assisted digestion in closed Teflon vessels). After cooling to room temperature the digest was diluted with MQ water and concentrations of B were determined by ICP-SFMS using a combination of internal standardization and external calibration. Elemental analysis was carried out in the medium resolution range, $\Delta m/m = 4500$ (Finnigan MAT, Bremen, Germany). Each measurement was done in triplicate.

(43) Hoegberg, E. I.; Cassaday, J. T. *J. Am. Chem. Soc.* **1951**, *73*, 557–559.

(44) Lefferts, J. L.; Molloy, K. C.; Zuckerman, J. J.; Haiduc, I.; Curtui, M.; Guta, C.; Ruse, D. *Inorg. Chem.* **1980**, *19* (10), 2862–2868.

(45) Bingham, A. L.; Drake, J. E.; Light, M. E.; Nirwan, M.; Ratnani, R. *Polyhedron* **2006**, *25*, 945–952.

(46) Colclough, T. *Ind. Eng. Chem. Res.* **1987**, *26*, 1888–1895.

(47) Singh, O. P.; Mehrotra, R. K.; Srivastava, G. *Phosphorus Sulphur Silicon* **1991**, *60*, 147–158.

(48) Lu, Z.; Chen, S.; Yu, Y.; Sun, J.; Xiang, S. *J. Therm. Anal. Cal.* **1999**, *55*, 197–203.

(49) Bedi, R. K.; Singh, I. *ACS Appl. Mater. Interfaces* **2010**, *2* (5), 1361–1368.

(50) Dickert, J. J.; Rowe, C. N. *J. Org. Chem.* **1967**, *32*, 647–653.

(51) Bansal, V.; Dohhen, K. C.; Sarin, R.; Sarpal, A. S.; Bhatnagar, A. K. *Tribol. Int.* **2002**, *35*, 819–828.

(52) Muller, N.; Lanterbur, P. C.; Goldenson, J. *J. Am. Chem. Soc.* **1956**, *7*, 3557–3561.

(53) Al-Malaika, S.; Coker, M.; Smith, P. J.; Scott, G. *J. Appl. Polym. Sci.* **1992**, *44*, 1297–1305.

(54) Villa, M.; Carduner, K. R.; Chiotelli, G. *J. Solid State Chem.* **1987**, *69*, 19–23.

(55) Mudrakowskii, I. L.; Shmachkova, V. P.; Kotsarenko, N. S.; Mastikhin, V. M. *J. Phys. Chem. Solids* **1986**, *47*, 335–339.

(56) Johnson, B. B.; Ivanov, A. V.; Antzutkin, O. N.; Forsling, W. *Langmuir* **2002**, *18*, 1104–1111.

(57) Zhang, L.; Eckert, H. *J. Mater. Chem.* **2005**, *15*, 1640–1653.

(58) Zielniok, D.; Cramer, C.; Eckert, H. *Chem. Mater.* **2007**, *19*, 3162–3170.

(59) Varlot, K.; Martin, J. M.; Grossiord, C.; Vargiolu, R.; Vacher, B.; Inoue, K. *Tribol. Lett.* **1999**, *6*, 181–189.

(60) Li, Y. R.; Pereira, G.; Lachenwitzer, A.; Kasrai, M.; Norton, P. R. *Tribol. Lett.* **2008**, *29*, 11–20.

(61) Fan, K.; Li, J.; Ma, H.; Wu, H.; Ren, T.; Kasrai, M.; Bancroft, G. M. *Tribol. Int.* **2008**, *41*, 1226–1231.

(62) Tao, M.; Liang, Y.; Xia, Y.; Zhou, F. *ACS Appl. Mater. Interfaces* **2009**, *1*, 467–471.

(63) Tse, J. S. *Nature* **2009**, *457*, 800–801.

(64) Oganov, A. R.; Chen, J.; Gatti, C.; Ma, Y.; Ma, Y.; Glass, C. W.; Liu, Z.; Yu, T.; Kurakevych, O. O.; Solozhenko, V. L. *Nature* **2009**, *457*, 863–867.